Regenerated fiber Bragg grating for fiber laser sensing at high temperatures

Yumin Zhang (张钰民)[1,2], Dandan Rong (戎丹丹)[1,2], Lianqing Zhu (祝连庆)[1,2,*], Mingli Dong (董明利)[1,2], and Fei Luo (骆 飞)[1]

[1]*Beijing Engineering Research Center of Optoelectronic Information and Instrument, Beijing Information Science and Technology University, Beijing 100016, China*

[2]*Beijing Key Laboratory of Optoelectronic Measurement Technology, Beijing Information Science and Technology University, Beijing 100192, China*

**Corresponding author: zhulianqing@sina.com*

Received November 26, 2017; accepted February 11, 2018; posted online March 30, 2018

Thermally regenerated low-reflectivity fiber Bragg gratings (RFBGs), as one mirror of a resonant cavity, have been introduced as linear-cavity fiber lasers combining with fiber saturable absorbers. The output of lasing presents an optical signal-to-noise ratio of 50 dB and temperature sensitivity coefficient of 15.36 pm/°C for the heating process and 15.46 pm/°C for the cooling process. The lasing wavelength variation and power fluctuation at 700°C are less than 0.02 nm and 0.21 dB, respectively. The RFBG-based fiber laser sensing has displayed good linearity for both the temperature rising and cooling processes, and favorable stability at high temperatures.

OCIS codes: 060.2370, 140.3510.
doi: 10.3788/COL201816.040606.

Fiber Bragg gratings (FBGs) are extensively used in the measurement of temperature, strain, displacement, vibration, and similar physical quantities[1–3]. Compared with FBGs, fiber lasers are powerful approaches for some sensing applications; they normally show overwhelming performance in terms of accuracy, sensitivity, and signal-to-noise ratio (SNR)[4]. The feature of high SNR and intensity makes fiber lasers especially useful for long-distance or extreme-conditions sensing. Recent research efforts have extended the operational measurement of high temperatures up to 1000°C using optical sensing[5]. The successful development of high-temperature sensing relies on high-temperature-resistant FBGs. Baker *et al.*[6] reported the peak reflectance degradation of a type I FBG when the temperature was above 295°C. It is indicated that the conventional FBG is limited if the temperature range is more than 300°C. The type II FBG inscribed by the femtosecond IR laser has overwhelming predominance in thermal stability. It is exploited to write FBGs in optical fibers without the requirement of material photosensitivity, which makes it a promising candidate for harsh-environment optical sensing. In 2004, the direct point-by-point inscription of an FBG by a femtosecond laser was reported by Bennion's group[7]. The obtained FBG was stable at the temperature reaching up to 900°C. A chemical composition grating, now often called a regenerated FBG, is the other alternative for high-temperature sensing. It was first presented by Fokine *et al.* in 2002[8]. The regenerated FBG can withstand temperatures up to 1200°C. There are several impressive examples of FBG thermal regeneration[9–12]. However, there is not a consensus about the understanding of the mechanisms underlying the grating regeneration, and different opinions on the matter do exist[13], such as the seeded crystallization model and the trapped water molecules model[14,15], but it does not affect the applications of regenerated FBGs at some specific areas.

The regenerated FBGs usually have a low reflectivity after thermal regeneration, even for strongly saturated seed gratings[16]. The low reflectivity brings a low SNR and affects the accuracy of interrogating, which has hindered the development of RFBGs in some precise sensing. Especially for the long-distance monitoring, the RFBGs could not play the high-temperature resistance potential. Introducing FBGs into a fiber laser system might be an effective solution. Chen *et al.*[17] presented a thermally regenerated distributed-Bragg-reflector (DBR) fiber laser for high-temperature operation up to 750°C. In 2008, Guan *et al.*[18] fabricated a DBR laser by directly inscribing highly saturated FBGs in an Er/Yb co-doped fiber and obtained a temperature resistance of 500°C. Ran *et al.*[19] reported an ultrashort DBR fiber laser based on a type II FBG with a temperature operation of 600°C. However, using a single low-reflectivity regenerated FBG for fiber laser sensing is seldom reported.

In this Letter, we present studies and characterization of a high-temperature stable fiber laser using a low-reflectivity regenerated FBG combined with a length of saturable absorber. The regenerated FBG is used as one of the resonant cavity for the fiber laser. The transmittance spectra were monitored during the regenerating process using a linear fiber laser system. The laser performance was characterized from 800°C to 300°C after the regeneration, and from 300°C to 800°C for the rising process. Continuous monitoring for the lasing power and wavelength fluctuation was performed to evaluate its stability

at 700°C. It was found that the regenerated FBG-contained fiber laser could measure high temperatures in conditions of high SNR and stability and had an extensive application prospect in long-distance sensing.

Fiber-saturable absorbers are extensively used in single-longitudinal-mode fiber lasers[20,21]. They are usually composed of a length of unpumped active optical fiber inserted into the fiber laser resonant cavity. In this Letter, a mode-selecting element composed by a Sagnac loop incorporated with unpumped erbium-doped fiber (EDF) is adopted. The incident light is split into two identical waves by the 3 dB coupler forming the Sagnac loop. The two counterpropagate waves in the unpumped EDF, form a standing wave that can be treated as an equivalent FBG. To be specific, the intensity along the saturable absorber will be periodically modulated. The absorption of laser emission in the location where the intensity is strong is easily saturated and the absorption coefficient is small, while the absorption coefficient of laser emission is large in the section where the intensity is weak. Therefore, a periodic distribution of the absorption coefficient is formed along the axial direction in the unpumped EDF. The full width at half-maximum bandwidth of the induced FBG can be written as[22]

$$\Delta f = \frac{c}{\lambda}\kappa\sqrt{\left(\frac{\Delta n}{2n_{\text{eff}}}\right)^2 + \left(\frac{1}{N}\right)^2}, \tag{1}$$

where $\kappa = 2\Delta n/(n_{\text{eff}}\lambda)$ is the coupling coefficient of the induced FBG; $N = L_g/\Lambda$ is the total number of grating periods; $\Lambda = \lambda/(2n_{\text{eff}})$ is the period of the induced FBG; λ is the central wavelength at which maximum reflectivity occurs; n_{eff} is the effective refractive index of the saturable absorber; Δn is the refractive index modulation depth of the saturable absorber; and L_g, c are the induced FBG length and velocity of light, respectively.

If $\lambda = 1555$ nm, $L_g = 2.5$ m, $n_{\text{eff}} = 1.45$, and $\Delta n \approx 3 \times 10^{-7}$, the bandwidth of the Sagnac loop with induced FBG will be calculated as $\Delta f = 12.2$ MHz. Considering the 14.8 MHz longitudinal mode interval of the fiber laser linear cavity, the mode-selection condition is well satisfied. This configuration will help to stabilize the lasing wavelength and power.

According to the Bragg equation, the shift of the Bragg wavelength caused by temperature can be expressed as

$$\Delta\lambda_B = (\xi + \alpha)\lambda_B \Delta T = K_T \Delta T, \tag{2}$$

where ξ and α are the thermo-optical coefficient and thermal expansion coefficient, respectively. K_T is the temperature sensitivity coefficient. The RFBG serves as the high-temperature sensing element whose wavelength determines the lasing wavelength. Therefore, the lasing wavelength is a function of temperature.

The schematic of the proposed high-temperature fiber laser sensing system is shown in Fig. 1. To achieve the measurement of the transmittance spectra of the RFBG and the fiber laser output wavelength, a linear-cavity fiber laser system is proposed. The system is composed of a pumping laser diode, a wavelength division multiplexer (WDM), a length of erbium-doped fiber (7 m, EDFC-980-HP, manufactured by Nufern), a muffle furnace, an FBG, a 3 dB coupler, a length of saturable absorber (2.5 m, EDFC-980-HP, manufactured by Nufern), and an optical spectrum analyzer (OSA). The transmittance spectra of the FBGs and lasing spectra were measured and recorded by the OSA (Yokogawa, AQ6370D) with a resolution of 0.02 nm. The heating range of the muffle furnace is from 25°C to 1100°C, with a temperature accuracy of ±1°C. A K-type thermocouple is placed near the location where the grating region of the FBG is fixed, and the value of temperature can be displayed on the thermometer with a temperature accuracy of ±0.6°C.

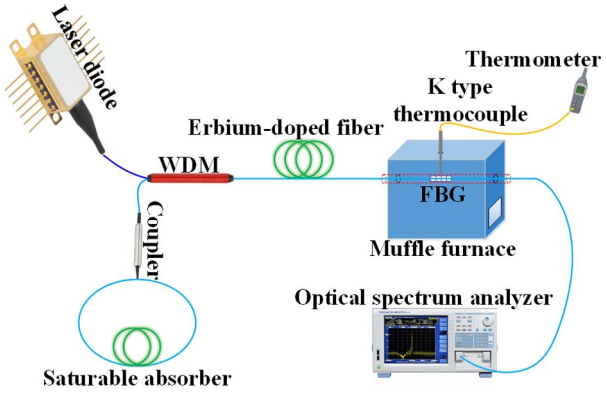

Fig. 1. Schematic of the experimental setup for the high-temperature fiber laser sensing system.

The FBG was written in SMF-28e optical fiber by an ultraviolet argon ion laser with a wavelength of 244 nm. The SMF-28e optical fiber was hydrogen-loaded prior to the grating writing ($P = 1750$ psi, $T = 80$°C, $t = 3$ days). Apodized FBG was inscribed into the optical fiber by scanning beam writing through an optical phase mask over 10 mm. The initial reflection and transmission spectra of the FBG are shown in Fig. 2. The peak wavelength is 1555.448 nm, and the depth of transmission is 30.73 dB, with a 3 dB reflection bandwidth of 0.3243 nm.

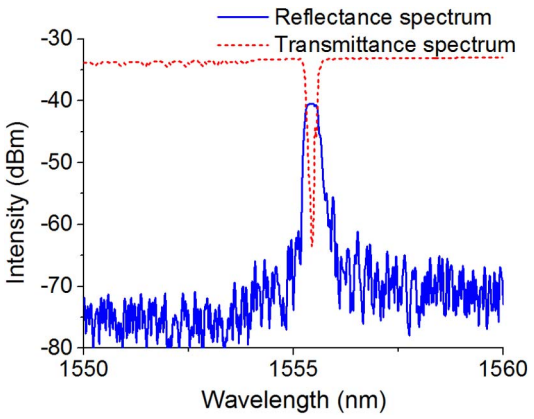

Fig. 2. Reflectance spectrum and transmittance spectrum of the seed grating for thermal regeneration.

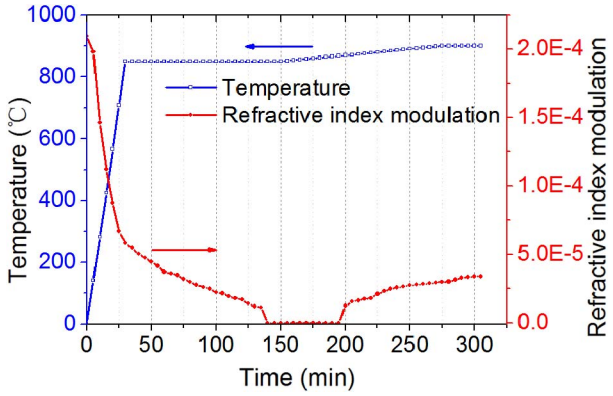

Fig. 3. Evolution of the refractive index modulation during the regeneration experiment.

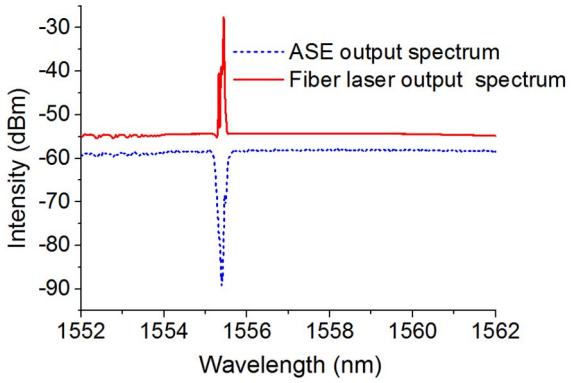

Fig. 4. ASE output spectrum and the fiber laser output spectrum before the thermal generation.

The thermal processing recipe for regenerating the FBG is shown in Fig. 3. First, the temperature is increased to 850°C uniformly from room temperature, and the heating rate is 28.3°C/min. For a period $t = 120$ min at 850°C, the FBG decays completely before regenerating. Second, the temperature slowly rises up to 900°C in 120 min. After a duration of about 60 min for disappearance of the FBG transmission spectrum, the FBG regenerates gradually during the heating process. Third, the dwell time at the temperature of 900°C is about 30 min until the stable appearance of the FBG spectrum.

During the regeneration, no weight was applied to the optical fiber. The evolution of the strength of the refractive index modulation of the FBG during the regeneration measurement is depicted in Fig. 3. Δn of the FBG decays at elevated temperatures. At the latter half of the holding period at 850°C, the transmittance spectrum of the FBG vanishes into the noise level, and a few minutes later the transmittance peak gradually gets stronger and the grating regenerates. To stabilize and accelerate the regeneration process, a slow heating plan with a temperature rising up to 900°C was adopted after the disappearance of the reflection spectrum. At 900°C the ultimate effective refractive index modulation of the RFBG is 3.39×10^{-5} and stabilizes at that value.

A linear cavity of an erbium-doped fiber laser was adopted for sensing under high temperature. The resonant cavity was composed of a total-reflection mirror (namely, the 3 dB coupler) and an FBG. The FBG was used as the output mirror and the sensing element after the regeneration process. The merit of the abovementioned structure was that it could not only measure the transmittance spectrum during the regeneration process but could also detect the output wavelength of the linear-cavity fiber laser. Before the FBG regeneration, the FBG and the 3 dB coupler make up a high-reflectivity resonant cavity. In this case, the threshold of the fiber laser system is relatively high because the radiation energy caused by pumping forms multiple reflections among the resonant cavity and rare parts of laser outputs from the port of FBG that are linked. Noting that the bandwidths of the FBG are somewhat wide and the forming fiber lasers are in multiple longitudinal mode, as shown in Fig. 4. When the laser diode driving current is below the threshold of the fiber laser, the fiber laser system becomes an amplified spontaneous emission (ASE). Therefore, the emission from the port of the FBG linked would be an ASE spectrum, and a transmittance spectrum can be obtained from that port, as shown in Fig. 4.

After the thermal regeneration process, the lasing characterization of the fiber laser was performed in the muffle furnace. The laser performance was characterized between 300°C and 800°C, which is 100°C below the regeneration temperature. Figure 5 depicts the lasing wavelength dependence on temperature. It can be seen that the output signal-to-noise ratio is ~50 dB, and the lasing shapes are all normal under different temperatures. To study high-temperature performance of the fiber laser, heating and cooling cycles between 300°C and 800°C were carried out. In the cooling process, the temperature of the muffle furnace was cooled from 800°C to 300°C with a temperature interval of 100°C, and the output laser varies from long wavelength to short wavelength, as shown in Fig. 6. The lasing wavelength shifted linearly as a function of temperature, and the sensitivity coefficient is

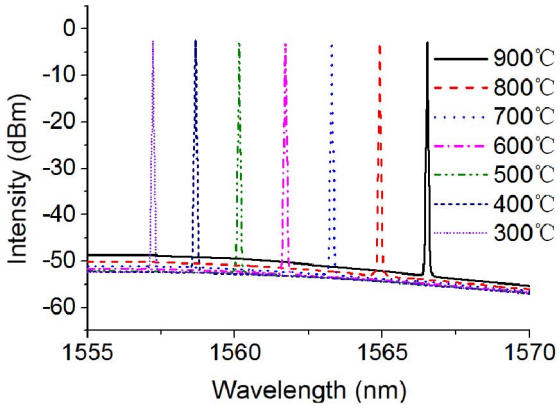

Fig. 5. Lasing wavelength evolution at different high temperatures.

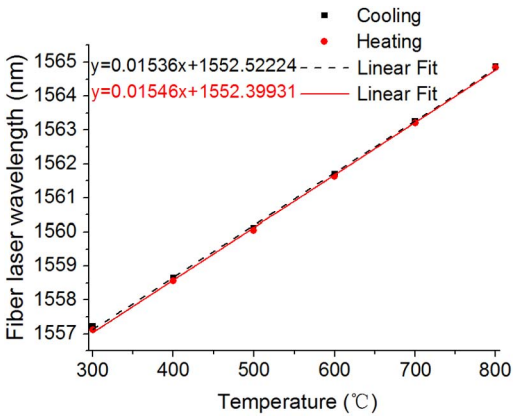

Fig. 6. Thermal wavelength shift of the fiber laser output and its linear fitting curves during the cooling and heating process.

15.36 nm/°C. While in the heating process, the temperature of the muffle furnace was heated from 300°C to 800°C with a temperature interval of 100°C. The lasing wavelength shifted linearly as a function of temperature, and the sensitivity coefficient is 15.46 nm/°C. As Fig. 6 illustrates, the fiber laser wavelengths match well for the cooling and heating process at high temperature, and the lasing wavelength differs relatively a little bigger at 300°C for the cooling and heating process than that at 800°C. The temperature drifts of the muffle furnace are slightly larger at low temperatures than those at high temperatures, which would be a possible reason for the difference of sensitivity coefficient during the cooling and heating process.

The reflectance spectrum of the RFBG and its laser spectrum are tested at room temperature using a broadband ASE source and the abovementioned fiber laser system, as shown in Fig. 7. The reflectivity of the RFBG is about 31.6%, and the signal-to-noise ratio of the fiber laser has overwhelming superiority compared with that of the RFBG.

The laser performance was further studied under high temperatures. The thermal stability of the laser output power at 700°C is exhibited in Fig. 8. The output power

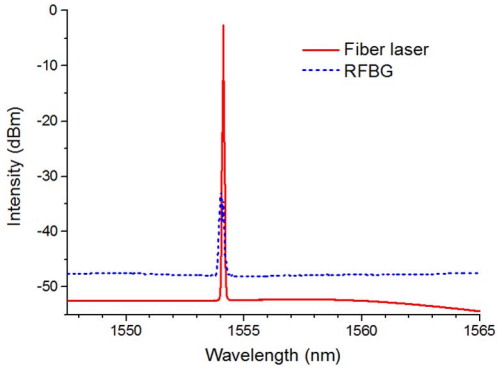

Fig. 7. Reflectance spectrum of the RFBG and its laser spectrum after the regeneration.

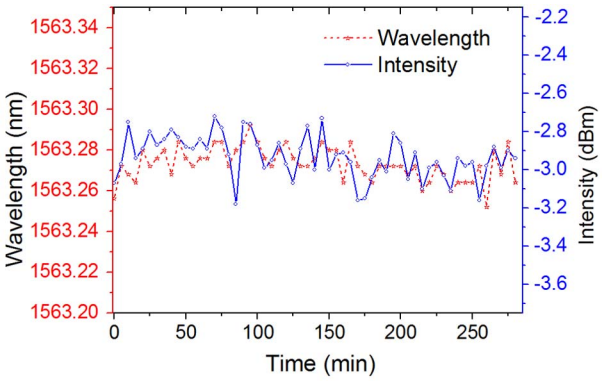

Fig. 8. Wavelength evolution and power stability of the fiber laser at 700°C.

presents stabilization tendency as the time goes on. The average power is −2.93 dBm with a standard deviation of ∼0.11. No decays in laser power were observed after 280 min of annealing. The lasing wavelength fluctuation was also carried out for the period of 280 min. It can be seen that the mean wavelength is 1563.273 nm and the standard deviation is 0.008, which indicates that the RFBG-based fiber laser is capable of sensing under high temperatures.

In conclusion, thermal regeneration of a UV-written FBG has been employed to measure high temperatures in a linear-cavity fiber laser. A combination of proper regenerating process and saturable absorber is adopted to stabilize the lasing performance at high temperatures. Good performance in terms of sensitivity and linearity, and favorable stability of lasing wavelength and power are achieved under high temperatures. Such RFBG-contained fiber lasers could be used for high-temperature sensing applications.

This work was supported by the Beijing Outstanding Talent Training Funded Project (No. 2015000020124G074), the 111 Project (No. D17021), and the Changjiang Scholars and Innovative Research Team in University (No. IRT_16R07).

References

1. Z. Y. Xu, Y. H. Li, and L. J. Wang, Photon. Res. **4**, 45 (2016).
2. Z. Liu and H. Tam, Chin. Opt. Lett. **14**, 120007 (2016).
3. Y. Pan, J. Jiang, W. Lu, H. Yang, K. Liu, S. Wang, H. Wang, and T. Liu, Chin. Opt. Lett. **15**, 070605 (2017).
4. Z. Yin, L. Gao, S. Liu, L. Zhang, F. Wu, L. Chen, and X. Chen, J. Lightwave Technol. **28**, 3403 (2010).
5. M. V. Reddy, K. Srimannarayana, R. L. N. S. Prasad, T. V. Apparao, and P. V. Rao, Proc. SPIE **9506**, 95060C (2015).
6. S. R. Baker, H. N. Rourke, V. Baker, and D. Goodchild, J. Lightwave Technol. **15**, 1470 (1997).
7. A. Martinez, M. Dubov, I. Khrushchev, and I. Bennion, Electron. Lett. **40**, 1170 (2004).
8. M. Fokine, Opt. Lett. **27**, 1016 (2002).
9. L. Shao, T. Wang, J. Canning, K. Cook, and H. Tam, Appl. Opt. **51**, 7165 (2012).
10. T. Wang, L. Shao, J. Canning, and K. Cook, Appl. Opt. **52**, 2080 (2013).

11. H. Yang, W. Y. Chong, Y. K. Cheong, K. Lim, C. H. Pua, S. W. Harun, and H. Ahmad, IEEE Sens. J. **13**, 2581 (2013).
12. A. Bueno, D. Kinet, P. Mégret, and C. Caucheteur, Opt. Lett. **38**, 4178 (2013).
13. P. Holmberg, F. Laurell, and M. Fokine, Opt. Express **23**, 27520 (2015).
14. J. Canning, M. Stevenson, S. Bandyopadhyay, and K. Cook, Sensors **8**, 6448 (2008).
15. B. Zhang and M. Kahrizi, IEEE Sens. J. **7**, 586 (2007).
16. V. Oliveira and H. J. Kalinowski, Proc. SPIE **7653**, 765301 (2010).
17. R. Chen, A. Yan, M. Li, T. Chen, Q. Wang, J. Canning, K. Cook, and K. P. Chen, Opt. Lett. **38**, 2490 (2013).
18. B. Guan, Y. Zhang, H. Wang, D. Chen, and H. Tam, Opt. Express **16**, 2958 (2008).
19. Y. Ran, F. Feng, Y. Liang, L. Jin, and B. Guan, Opt. Lett. **40**, 5706 (2015).
20. J. Lee, M. Jung, M. Melkumov, V. F. Khopin, E. M. Dianov, and J. H. Lee, Laser Phys. Lett. **14**, 065104 (2017).
21. J. Zhao, C. Zhang, C. Miao, and H. Gu, Opt. Commun. **331**, 229 (2014).
22. K. Zhang and J. U. Kang, Opt. Express **16**, 14173 (2008).